Cdon Mutation and Fetal Alcohol Converge on Nodal Signaling in a Gene-Environment Interaction Model of Holoprosencephaly

Mingi Hong[1], Annabel Christ[2], Anna Christa[2], Thomas E. Willnow[2], and Robert S. Krauss[1,*]

[1]Department of Cell, Developmental, and Regenerative Biology, Icahn School of Medicine at Mount Sinai, New York, NY 10029, USA; [2]Max-Delbruck-Center for Molecular Medicine, 13125 Berlin, Germany

*Corresponding Author:

Robert S. Krauss, Department of Cell, Developmental, and Regenerative Biology, Icahn School of Medicine at Mount Sinai, New York, NY 10029. Phone: 212-241-2177; Fax: 212-860-9279; e-mail: Robert.Krauss@mssm.edu

SUMMARY

Holoprosencephaly (HPE), a failure to define the midline of the forebrain and midface, arises in ~1 in 250 conceptions. It is associated with predisposing mutations in the Nodal and Hedgehog (HH) pathways, with penetrance and expressivity graded by genetic and environmental modifiers that work via poorly understood mechanisms. CDON is a multifunctional co-receptor, including for the HH pathway. In mice, *Cdon* mutation synergizes with fetal alcohol exposure to produce HPE phenotypes closely resembling those seen in humans. We report here that, unexpectedly, Nodal, not HH, signaling is the point of synergistic interaction between mutation of *Cdon* and fetal alcohol exposure. A combination of window-of-sensitivity, genetic, and *in vitro* findings are consistent with a model whereby CDON and another auxiliary receptor, LRP2, function to regulate the Nodal pathway, with consequent effects on downstream HH signaling during midline patterning. Brief exposure of *Cdon* mutant embryos to ethanol during this period transiently and partially inhibits Nodal pathway activity. These results illuminate mechanisms of gene-environment interaction in a multifactorial model of a common birth defect.

INTRODUCTION

It is thought that many common structural birth defects are caused by a complex and ill-defined combination of genetic and environmental factors (Krauss and Hong, 2016). The notion that environmental agents can affect the penetrance and expressivity of predisposing mutations is speculated to underlie many human congenital anomalies, but has been difficult to demonstrate in human populations. Animal models are therefore required, but these have been slow to emerge. Some recent successful examples are a zebrafish model of craniofacial defects (*Pdgfra* mutations and fetal alcohol), and mouse models of scoliosis (Notch pathway mutations plus hypoxia), facial clefting (*Pax3* mutations plus 2,3,7,8-tetrachlorodibenzodioxin (TCDD)), and holoprosencephaly (Hedgehog pathway mutations and fetal alcohol) (Hong and Krauss, 2012; Kietzman et al., 2014; McCarthy et al., 2013; Sparrow et al., 2012; Zalc et al., 2015).

Holoprosencephaly (HPE) is a common developmental defect in midline patterning of the forebrain and/or midface (Muenke and Beachy, 2001). HPE occurs approximately once per 250 human conceptions, with an associated in utero lethality of ~97% (Leoncini et al., 2008; Shiota and Yamada, 2010). HPE is characterized by an unbroken continuum of rostroventral midline anomalies that range from complete failure to partition the forebrain into hemispheres plus cyclopia, through progressively less severe defects including partially partitioned forebrain, single nostril, midface hypoplasia, and single central maxillary incisor (Cohen, 2006; Krauss, 2007; Muenke and Beachy, 2001).

Development of the rostroventral midline is initiated by signals derived from the prechordal plate (PCP) (Kiecker and Niehrs, 2001; Marcucio et al., 2011). The PCP produces the morphogen Sonic hedgehog (SHH), initiating a sequence of events that progressively patterns the forebrain and midface. *Shh* is expressed in a temporal cascade: first in the PCP, subsequently in the ventral midline of the diencephalon and telencephalon, and finally in the midfacial ectoderm (Aoto et al., 2009; Cordero et al., 2004; Geng and Oliver, 2009; Kiecker and Niehrs, 2001; Rubenstein and Beachy, 1998; Zhang et al., 2006). SHH induces midline cell fates and structures throughout this period. HH ligands initiate signaling by binding the primary receptor Patched1 (PTCH1). In the absence of ligand, PTCH1 constrains the activity of a second membrane protein, Smoothened (SMO). HH binding inhibits PTCH1 function, allowing SMO-dependent signals to activate GLI transcription factors and pathway-specific gene expression. HH ligand availability and signal reception are also regulated by a series of co-receptors and additional HH-binding proteins, including CDON, BOC, GAS1, and LRP2 (Beachy et al., 2010; Kong et al., 2019; Lee et al., 2016; Petrov et al., 2017; Willnow and Christ, 2017).

The PCP develops from the anterior primitive streak (APS) under the influence of Nodal pathway signaling (Robertson, 2014; Schier, 2009; Shen, 2007). Therefore, the Nodal pathway is developmentally upstream of the HH pathway in rostroventral midline patterning. Consistent with this conclusion, defective Nodal signaling at the primitive streak stage of development leads to defects in HH signaling and HPE (Krauss, 2007). Nodal is a TGFβ superfamily member and signals through a receptor complex including the type I and type II receptors, ALK4 and Activin receptor IIA/B (ActRIIA/B), and a GPI-

linked co-receptor, Cripto (Robertson, 2014; Schier, 2009; Shen, 2007). Receptor activation results in phosphorylation of the transcription factors SMAD2 and SMAD3, which interact with another transcription factor, FOXH1, to activate genes required for PCP induction (Robertson, 2014; Schier, 2009; Shen, 2007). Among these genes are *FoxA2* and *Gsc* (Ang and Rossant, 1994; Belo et al., 1998; Filosa et al., 1997). Nodal signaling also induces expression of *Lefty1* and *Lefty2*, which encode secreted inhibitors of the pathway that bind to Cripto and Nodal itself (Robertson, 2014; Schier, 2009; Shen, 2007).

The etiology of HPE is complex, involving both genetic and environmental risk factors (Hong and Krauss, 2018; Johnson and Rasmussen, 2010; Krauss, 2007; Miller et al., 2010; Muenke and Beachy, 2001; Roessler et al., 2018a; Roessler et al., 2018b; Summers et al., 2018). Heterozygous, loss-of-function mutations in components or regulators of the HH and Nodal signaling pathways are associated with HPE (Roessler et al., 2018a; Roessler et al., 2018b). Epidemiology of HPE is less advanced than genetic analyses, but among the environmental risk factors implicated is fetal alcohol exposure (Abe et al., 2018; Cohen and Shiota, 2002; Croen et al., 2000). A full range of clinical phenotypes is observed in both sporadic and familial HPE (Muenke and Beachy, 2001; Solomon et al., 2010). Many mutation carriers in pedigrees lack clinical manifestation, and many apparently sporadic cases have inherited a mutation from a minimally affected parent (Lacbawan et al., 2009; Solomon et al., 2012). It is likely, therefore, that HPE-associated mutations are not sufficient to produce midline defects, but are the substrate on which a complex landscape of genetic and/or environmental modifiers act. Statistical analysis is consistent with a multifactorial, “autosomal dominant

with modifier" model, wherein the penetrance and expressivity of a heterozygous driver mutation is graded by the modifier landscape (Hong and Krauss, 2018; Roessler et al., 2012).

We have modeled this phenomenon in mice with high fidelity. *CDON* encodes a multi-functional co-receptor, including for the HH pathway, (Lu and Krauss, 2010; Sanchez-Arrones et al., 2012), and *CDON* mutations are associated with human HPE (Bae et al., 2011; Roessler et al., 2018a). *Cdon*$^{-/-}$ mice on a 129S6 genetic background have a subthreshold defect in HH signaling and are subject to HPE induced by genetic and environmental modifiers; among the latter is ethanol (EtOH) (Hong and Krauss, 2018). *Cdon* mutation or in utero EtOH exposure individually yielded little effect on 129S6 mice; the combination, however, synergized to inhibit HH signaling in the developing forebrain and produced a complete spectrum of HPE phenotypes with high penetrance (Hong and Krauss, 2012). Furthermore, fetal EtOH induces a low penetrance of HPE in C57BL/6J mice, and this was exacerbated by heterozygosity for *Shh* or *Gli2* (Kietzman et al., 2014). Consistent with the notion that a threshold of HH signaling activity is rate-limiting in midline patterning, genetic removal of one copy of the negative pathway regulator, *Ptch1*, rescued 129S6 *Cdon*$^{-/-}$ mice from EtOH-induced HPE (Hong and Krauss, 2013).

It is possible that EtOH interferes directly with HH signaling. However, defective HH pathway function may be a final common mechanism for all classical forms of HPE, so these results do not prove that HH signaling is the direct synergistic target of *Cdon* mutation and in utero EtOH exposure. Alcohol toxicity is often associated with its oxidative metabolism (Heit et al., 2015). However, several lines of experimental

evidence argue that EtOH itself, rather than a consequence of its metabolism, is the HPE-inducing teratogen (Hong and Krauss, 2017). In this study, we demonstrate that the window of sensitivity to EtOH-induced HPE in 129S6 *Cdon*$^{-/-}$ mice is closed by embryonic day (E) 7.5, prior to *Shh* expression in the PCP (Echelard et al., 1993). The sensitivity period of EtOH-induced HPE overlaps with Nodal-mediated specification of the PCP from the APS. In addition to serving as a HH co-receptor, we find that CDON interacts genetically and physically with regulators of Nodal signaling. Furthermore, EtOH inhibits Activin/Nodal pathway signaling *in vitro* in mouse epiblast stem cells (mEpiSCs), which have transcriptional and functional properties that resemble APS cells (Kojima et al., 2014; Tsakiridis et al., 2014). Together these results argue that, unexpectedly, *Cdon* mutation and fetal alcohol synergize to induce HPE by interfering with Nodal signaling. These results illuminate mechanisms of gene-environment interaction in a high fidelity, multifactorial model of a common birth defect.

RESULTS

The Window of Sensitivity to EtOH-Induced HPE Coincides with Nodal, not HH, Signaling

All studies with EtOH were performed with mice on a 129S6 background and are referred to only by genotype unless otherwise noted. Our model uses one-hour timed mating of *Cdon*$^{+/-}$ mice, allowing rigorous identification of a window of sensitivity for EtOH's teratogenic effects. The EtOH treatment regimen involves one dose at E7.0 and a second dose four hours later; this results in a full range of HPE phenotypes in *Cdon*$^{-/-}$ mice with overall penetrance of ~75% (Hong and Krauss, 2012). The protocol is analogous to the original regimen developed to model fetal alcohol spectrum disorders in C57BL/6J mice, wherein ~19% developed HPE phenotypes (Aoto et al., 2008; Sulik et al., 1981). HPE phenotypes were not induced in wild type C57BL/6J mice when EtOH was administered at E6.5 or E7.5 (Aoto et al., 2008). We have shown that EtOH is ineffective in *Cdon*$^{-/-}$ mice when administered at E8.0 (Hong and Krauss, 2012). To further refine the temporal window of sensitivity, we assessed the ability of EtOH to induce HPE in *Cdon*$^{-/-}$ animals when administered at E7.25 and E7.5, with mice examined at E14.0. EtOH was effective at E7.25, but not at E7.5 (Table 1).

EtOH itself is the HPE-inducing teratogen in this system (Hong and Krauss, 2017). The developmental processes directly perturbed by EtOH must therefore occur: 1) during the sensitive time window; and 2) prior to EtOH clearance, even if defects in midline development occur later. *Shh* expression in the midline begins at E7.5-E7.75 (Echelard et al., 1993). When administered at E7.0, maternal blood EtOH levels peaked at E7.25 and were no longer detectable by ~E7.75 (Hong and Krauss, 2012). Critically,

EtOH is no longer effective at E7.5, a time prior to SHH function in midline patterning (Echelard et al., 1993; McMahon et al., 2003). Therefore, it is very unlikely that direct inhibition of HH signaling is the mechanism of EtOH-induced HPE. Consistent with this conclusion, the time of peak sensitivity to HPE induced by the direct SMO inhibitor Vismodegib was E7.5, 6 – 12 hours later than for EtOH (Heyne et al., 2015).

Both the window of sensitivity to EtOH and peak EtOH levels overlap with induction of the PCP by Nodal signaling. We previously observed that expression of *FoxA2* and *Gsc*, genes regulated by Nodal that mark the APS (from which the PCP is derived), was diminished at E7.25 in EtOH-treated *Cdon*$^{-/-}$ embryos. Both *Cdon* mutation and EtOH exposure were required for this effect (Hong and Krauss, 2012). Expression of *Lefty2*, a direct Nodal pathway target gene, was also reduced at E7.25 specifically in EtOH-treated *Cdon*$^{-/-}$ embryos (Figure 1). Taken together, these results showed that the synergy between loss of CDON and in utero EtOH exposure occurred during Nodal-dependent specification of the PCP and that reduction of Nodal target gene expression required a combination of mutation and teratogen. The observation that loss of CDON was required for the effect suggests that, in addition to its role as a SHH co-receptor, CDON functions earlier in development to promote midline patterning, potentially via the Nodal pathway. In fact, *Cdon* expression initiates during gastrulation and is seen in embryonic mesoderm and ectoderm (Hong and Krauss, 2012; Mulieri et al., 2000).

Cdon Interacts Genetically with Nodal Pathway Components

Mice with mutations resulting in complete loss of Nodal signaling gastrulate abnormally and die early in development, but hypomorphic pathway mutants display a range of HPE phenotypes (Andersson et al., 2006; Chu et al., 2005; Lowe et al., 2001; Nomura and Li, 1998; Schier, 2009; Shen, 2007; Song et al., 1999). To further probe the linkage between CDON and regulation of Nodal signaling, we assessed whether *Cdon* interacted genetically with *Cripto* and *Lefty2*, direct positive and negative regulators of the Nodal pathway, respectively. When analyzed at E10, ~14% of *Cdon*$^{-/-}$ embryos treated with EtOH had alobar HPE and cyclopia, dying in utero by E11 (Hong and Krauss, 2012, 2013). When studied at E14, ~70% of such embryos displayed lobar HPE and a range of craniofacial midline phenotypes, including fused upper lip and single nostril (Hong and Krauss, 2012, 2013). To address genetic interactions between *Cdon* and Nodal pathway regulators, we took advantage of the high penetrance of phenotypes at E14 and analyzed embryos at this stage for these unambiguous, easily scored phenotypes.

Targeted mutations in *Cripto* and *Lefty2* (Ding et al., 1998; Meno et al., 1999) were placed onto the 129S6 genetic background and then crossed to *Cdon* mutants to generate double heterozygotes. Offspring of intercrosses of these mice were further crossed and pregnant females were treated with EtOH or saline as a control. *Cripto* is essential for Nodal signaling. *Lefty2* is induced in response to Nodal signaling to provide critical negative feedback as an inhibitor of the pathway. Since CDON and EtOH may act together at the level of Nodal signaling in HPE, we predicted that removal of one copy of *Cripto* would sensitize *Cdon*$^{-/-}$ embryos to EtOH-induced HPE. In contrast, we

predicted that removal of one copy of *Lefty2* would rescue *Cdon*$^{-/-}$ embryos from EtOH-induced HPE. (Null mutations in *Cripto* and *Lefty2* result in early lethality due to strong gastrulation defects (Ding et al., 1998; Meno et al., 1999), so studying homozygous double mutants with *Cdon* is impossible.) To permit the detection of sensitization by *Cripto* heterozygosity, we used a dose of EtOH which we previously reported gives ~30% penetrance of HPE at E14 (2.9 g/kg) (Hong and Krauss, 2012). With this regimen, 28% of EtOH-treated *Cdon*$^{-/-}$*; Cripto*$^{+/+}$ embryos had HPE, whereas 55% of *Cdon*$^{-/-}$*;Cripto*$^{+/-}$ embryos did ($p<0.014$) (Table 2, Figure S1). With the exception of a single EtOH-treated *Cdon*$^{+/-}$*;Cripto*$^{+/-}$ embryo, EtOH-treated mice of other genotypes and saline-treated control mice did not display HPE. Removal of one copy of *Cripto* therefore sensitized *Cdon*$^{-/-}$ mice to EtOH-induced HPE.

Nodal$^{-/-}$ and *Lefty2*$^{-/-}$ embryos have opposite defects in gastrulation and display dosage-dependent genetic interactions, with *Lefty2* functioning as a negative regulator of the pathway (Meno et al., 1999). To test for phenotypic suppression in EtOH-induced HPE, we used the standard dose of EtOH (3.48 g/kg) for these analyses, as it results in high penetrance. All embryos with HPE at E14 display a fused upper lip, while only some of these show the more severe single nostril phenotype. Approximately 70% of EtOH-treated *Cdon*$^{-/-}$*; Lefty2*$^{+/+}$ embryos had a fused upper lip, similar to our previous findings (Hong and Krauss, 2012, 2013), whereas 54% of *Cdon*$^{-/-}$*;Lefty2*$^{+/-}$ embryos displayed HPE, revealing a trend toward overall reduction of HPE frequency ($p=0.14$). However, 21% of EtOH-treated *Cdon*$^{-/-}$*;Lefty2*$^{+/+}$ embryos had a single nostril, but only 6% of *Cdon*$^{-/-}$*; Lefty2*$^{+/-}$ embryos did ($p<0.05$) (Table 3, Figure S1). Again, EtOH-treated mice of other genotypes and saline-treated control mice did not display HPE. Therefore,

removal of one copy of *Lefty2* rescued the more severe form of HPE associated with EtOH treatment. Taken together, these studies revealed that the Nodal signaling components *Cripto* and *Lefty2* act as heterozygous enhancer and suppressor genes, respectively, of EtOH-induced HPE in *Cdon*$^{-/-}$ embryos.

EtOH Inhibits Activin/Nodal Signaling in mEpiSCs

The APS is a small, transiently existing cell population, making it hard to study directly. Cultured mEpiSCs have transcriptional and functional properties closely resembling APS cells (Kojima et al., 2014; Tsakiridis et al., 2014), making them a tractable *in vitro* surrogate model. mEpiSCs rely on FGF2 and Activin/Nodal signaling for maintenance as self-renewing, pluripotent stem cells (Brons et al., 2007; Vallier et al., 2009). Activin A and Nodal use the same receptor and signaling mechanism, except that Nodal, but not Activin A, requires the co-receptor Cripto. Therefore, we evaluated the effects of EtOH on Activin/Nodal signaling in mEpiSCs.

A direct readout of Nodal signaling activity is receptor-mediated phosphorylation of SMAD2 at its C-terminus (Robertson, 2014; Schier, 2009; Shen, 2007). We assessed C-terminally phosphorylated SMAD2 (p-SMAD2C) and total SMAD2 levels in the mEpiSC line, EpiSC9 (Najm et al., 2011), treated with EtOH for 6 hours. A relatively short treatment duration was chosen because: 1) the *in vivo* model is an acute exposure regimen; 2) the window of sensitivity to EtOH-induced HPE is <12 hours; and 3) high EtOH levels last only about 10 hours in pregnant females (Hong and Krauss, 2012). EtOH dose-dependently diminished p-SMAD2C levels in mEpiSCs, without altering total SMAD2 levels (Figure 2A, B).

EtOH stimulates activation of the MAP kinase, JNK, in specific cell types (McAlhany et al., 2000; Ren et al., 2017). SMAD2 can also be phosphorylated in its linker region by MAP kinases (Massagué, 2003; Rezaei et al., 2012), usually leading to inhibition of SMAD2 function (Grimm and Gurdon, 2002; Kretzschmar et al., 1999; Lessard et al., 2018). We therefore assessed total and phosphorylated (activated) forms of JNK1 MAP kinase in EtOH-treated mEpiSCs. EtOH dose-dependently increased phospho-JNK1 (T183/Y185) levels (p-JNK1; Figure 2A, B). Consistent with EtOH-induced p-JNK1 activation, phosphorylation of the SMAD2 linker region (p-SMAD2L) also occurred in an EtOH dose-dependent manner, with production of p-JNK1 and p-SMAD2L correlating tightly (Figure 2A, B). Reduction of p-SMAD2C, and elevation of p-SMAD2L, levels by acute EtOH exposure of mEpiSCs *in vitro* is consistent with EtOH's ability to inhibit Nodal pathway target gene expression in primitive streak stage *Cdon*$^{-/-}$ embryos.

Cdon and *Lrp2* Genetically Interact in Mice to Generate a Phenotype Similar to Nodal Pathway Hypomorphs, and Both Bind to Cripto

Our findings argue that CDON plays an earlier role in development than its known function as a SHH co-receptor. The need for EtOH exposure to reveal this role suggests that CDON's effects in primitive streak embryos may be redundant with other factors. The HH co-receptors BOC and GAS1 are not likely to be such factors, as *Cdon;Boc;Gas1* triple knockout mice had a phenotype that is close to a complete loss of embryonic HH pathway function, but not Nodal pathway-like phenotypes (Allen et al., 2011). LRP2 is an endocytic and auxiliary receptor for multiple morphogenetic ligands

and receptors (Willnow and Christ, 2017). *Lrp2*$^{-/-}$ mice have HPE of variable penetrance and severity (Christ et al., 2012; Spoelgen et al., 2005; Willnow and Christ, 2017; Willnow et al., 2012). We therefore constructed mice with mutations in *Cdon* and *Lrp2*. Some *Cdon;Lrp2* double mutants at E11.5 had a severe truncation of anterior head and face structures, a phenotype neither single mutant displayed (Figure 3A). Surviving embryos displayed a range of phenotypes, including milder craniofacial truncation and strong HPE (Figure 3B, C). Loss of anterior head structure is a more severe phenotype than that seen even in *Smo* mutants, which lack all HH signaling (Zhang et al., 2001). These phenotypes – anterior truncations and HPE – are similar to those observed in mice with partial loss of Nodal pathway function (e.g., hypomorphic *Nodal* and *Cripto* mutants, and *Nodal*$^{+/-}$*;Smad2*$^{+/-}$ mutants, each have phenotypes that include truncation of anterior head structures and severe HPE) (Andersson et al., 2006; Chu et al., 2005; Lowe et al., 2001; Nomura and Li, 1998; Song et al., 1999). The *Cdon*/*Lrp2* genetic interaction is specific and selective: the *Cdon* paralog *Boc* is not expressed in primitive streak-stage embryos (Mulieri et al., 2002; Zhang et al., 2001), and *Boc* mutant mice do not synergize with *Lrp2* mutants (unpublished results), nor are they sensitive to EtOH-induced HPE (Hong and Krauss, 2012).

CDON is a multifunctional co-receptor and promotes SHH-independent signaling when associated with various other receptors and cell adhesion molecules. In addition to binding HH ligands and PTCH1, CDON interacts with and influences signaling by classical cadherins; the netrin receptor, neogenin; and the WNT co-receptor, LRP6 (Bae et al., 2011; Bae et al., 2009; Izzi et al., 2011; Jeong et al., 2014; Kang et al., 2003; Kang et al., 2004; Lu and Krauss, 2010; Tenzen et al., 2006). We hypothesized that

CDON might work similarly in Nodal signaling. To address this possibility, we assessed whether CDON binds to Nodal receptor components. A secreted CDON ectodomain fused in-frame at its carboxy terminus with the IgG Fc region (CDON-Fc) was expressed in HEK293T cells with individual ectodomains of the Nodal receptor (ActRIIA, ActRIIB, ALK4, and Cripto) fused in-frame at their carboxy termini with alkaline phosphatase (AP). As positive and negative controls, SHH-N-AP and CD164-AP were used, respectively (SHH-N is the active portion of SHH, CD164 is a cell surface sialomucin) (Kang et al., 2002; Tenzen et al., 2006). The use of secreted ectodomains reduces the possibility that unknown, cell surface bound factors promote binding or contribute directly to the complex. Conditioned medium was collected, equivalent amounts of AP fusion proteins from conditioned media were pulled down and blotted for captured CDON-Fc. Conversely, equivalent levels of Fc were pulled down, and associated AP activity was quantified. Similar results were obtained in each pull-down: CDON-Fc interacted efficiently with Cripto-AP, similar to the interaction between CDON-Fc and SHH-N-AP (Figure 4A, B). CDON-Fc did not bind to the negative control CD164-AP, and it interacted only weakly with the AP-tagged versions of ALK4, ActRIIA, and ActRIIB (Figure 4A, B).

As CDON and LRP2 interact genetically to produce a Nodal hypomorph-like phenotype, we asked whether LRP2, like CDON, binds to Cripto. The extracellular region of LRP2 harbors four repetitive modules, each comprising a cluster of complement-type repeats followed by EGF-type repeats and β-propellers. Each module is likely capable of independently binding ligands, as shown for the related receptor, LRP1 (Croy et al., 2003). LRP2 is a huge polypeptide of 4660 amino acids, making it

difficult to express *in vitro*. Therefore, we constructed a series of soluble “mini-receptors” (designated sR1, sR2, sR3, and sR4) spanning virtually the entire ectodomain in four non-overlapping pieces, each fused in-frame at their carboxy termini to the IgG Fc region (see Figure 4C). Each soluble ectodomain segment and Cripto-AP were expressed in HEK293T cells and assessed for their ability to bind to each other. LRP2 binds SHH-N (Christ et al., 2012; McCarthy et al., 2002), so this ligand was used again as a positive control, with CD164-AP serving as a presumptive negative control. Each soluble LRP2 mini-receptor ectodomain (i.e., sR1 to sR4) pulled down SHH-N-AP, revealing that LRP2 harbors multiple SHH-N binding sites (Figure 4D). These results were confirmed by expressing each ectodomain segment joined with the native LRP2 transmembrane and cytoplasmic domains (mini-receptors R1, R2, R3, and R4; Figure 4C) in NIH3T3 cells. These cultures were incubated with recombinant SHH-N-GST fusion proteins for 2 hours, followed by immunoprecipitation with anti-LRP2 antibody recognizing all mini-receptors and Western blotting with antibodies to LRP2 or GST. Again, all four mini-receptors pulled down SHH-N, whereas no pulldown of SHH-N was seen in control transfectants lacking LRP2 mini-receptors (Figure 4E). Finally, we assessed LRP2 binding to Cripto with the soluble ectodomain binding assay. Similar to its multivalent interaction with SHH-N, each soluble LRP2 ectodomain segment (sR1 to sR4) pulled down Cripto-AP (Figure 4D). The efficiency of LRP2 mini-receptor ectodomains to bind SHH-N-AP and Cripto-AP was similar to that of CDON-Fc (Figure 4D).

DISCUSSION

HPE is one of the most common developmental defects, but its etiology remains poorly understood. Mutations in the Nodal, HH, and FGF signaling pathways are associated with HPE (Roessler et al., 2018a), but these alone are insufficient to drive aberrant development. Identifying and understanding the critical phenotypic modifiers of such mutations is important but still in its infancy. Many birth defects are thought to be caused by poorly defined interactions between genetic and environmental risk factors, but the mechanistic bases of these interactions are largely unknown (Krauss and Hong, 2016). *Cdon* mutation and fetal alcohol are each implicated in human HPE (Abe et al., 2018; Bae et al., 2011; Cohen and Shiota, 2002; Croen et al., 2000; Roessler et al., 2018a). The *Cdon* mutation plus fetal alcohol model was the first gene-environment interaction model for HPE, and it is noteworthy for its specificity and fidelity to many aspects of human HPE (Hong and Krauss, 2012). Therefore, illumination of how loss of *Cdon* interacts with in utero EtOH exposure provides insight into mechanisms of HPE and how fetal alcohol functions as a teratogen in this developmental defect.

The Nodal pathway is developmentally upstream from the HH pathway in patterning the rostroventral midline. While CDON is clearly a component of the HH pathway, it also regulates signaling within several additional pathways (Bae et al., 2011; Bae et al., 2009; Izzi et al., 2011; Jeong et al., 2014; Kang et al., 2003; Kang et al., 2004; Lu and Krauss, 2010; Tenzen et al., 2006). Multiple lines of evidence presented here argue that CDON also regulates Nodal signaling and that the Nodal pathway is the point of synergistic interaction between mutation of *Cdon* and fetal EtOH exposure. The evidence includes: 1) EtOH-treated *Cdon*$^{-/-}$ embryos display defects in expression of

Nodal target genes in the APS, whereas EtOH treatment or *Cdon* mutation alone do not; 2) the window of sensitivity to EtOH-induced HPE is very narrow and closed by E7.5, prior to *Shh* function in rostroventral midline patterning; 3) EtOH itself is the likely HPE-inducing teratogen and peak circulating EtOH levels coincide with Nodal signaling in the APS; 4) *Cdon* interacts genetically with the critical Nodal pathway factors *Cripto* and *Lefty2* in EtOH-induced HPE; 5) acute EtOH treatment dose-dependently diminishes p-SMAD2C and elevates p-SMAD2L levels in Activin/Nodal signaling-dependent mEpiSC cells; 6) *Cdon;Lrp2* double mutants display phenotypes similar to mice with hypomorphic Nodal pathway mutations, including anterior truncations, a phenotype not seen in mice lacking all HH signaling; and 7) CDON and LRP2 both bind efficiently to Cripto, an essential component of the Nodal receptor.

Taken together, our findings are consistent with the following model: CDON and LRP2 function with overlapping or compensatory roles to regulate Nodal pathway signaling in the APS during induction of the PCP. Brief exposure of *Cdon*$^{-/-}$ embryos to EtOH during this period transiently and partially inhibits Nodal pathway activity. While all the mice successfully gastrulate, they emerge from this period predisposed towards development of HPE in a stochastic manner. Subsequent defects in HH signaling are a consequence of both this phenomenon and the genetic lack of CDON function in the HH pathway later in development. If HH signaling strength fails to reach a required threshold early during rostroventral midline patterning, at the PCP stage, the outcome is alobar HPE and cyclopia; if it occurs at later stages of development, the outcomes are progressively less severe. Aspects of the model will require additional experimentation, but it is logically consistent with the synergistic effects of fetal alcohol and *Cdon*

mutation within a narrow window of sensitivity, and also with the “mutation plus modifier” view of human HPE.

The specific mechanisms whereby acute EtOH treatment reduces expression of Nodal target genes in the APS of *Cdon*$^{-/-}$ mice and diminishes p-SMAD2C levels in mEpiSCs are not known. EtOH itself, rather than consequences of its oxidative metabolism, is very likely the HPE-inducing teratogen (Hong and Krauss, 2017). An alternative mechanism to metabolism-based toxicity is that EtOH itself functions to perturb cell membranes via its hydrophobicity (Lyon et al., 1981; McCarns et al., 1997). One possibility is that EtOH’s hydrophobic nature results in destabilization of trafficking of Nodal receptor components or their stable assembly at the cell surface. Cripto is a GPI-linked protein, so might be especially vulnerable to hydrophobic membrane perturbation. However, exogenously provided Activin A is the major activator of Smad2 in cultured mEpiSCs, and Activin does not require Cripto to signal through ActRII/Alk4. EtOH reduces p-SMAD2C levels in these cultures, so Cripto may not be a direct critical target of EtOH. Nevertheless, mEpiSCs endogenously express Nodal (Kojima et al., 2014), which does require Cripto, and its contribution to SMAD2 signaling in these cultures is not fully clear. Additionally, EtOH activates JNK1 in mEpiSCs, with a corresponding increase in p-SMAD2L levels. Phosphorylation of SMAD2 by MAP kinases is generally inhibitory to SMAD2 activity, independent of p-SMAD2C phosphorylation status (Massagué, 2003; Rezaei et al., 2012), so EtOH appears to promote or inhibit multiple signals that converge on SMAD2 phosphorylation.

CDON regulates several signaling pathways, but it has not previously been implicated in Nodal signaling. Our findings reveal a new role for this multifunctional

protein. Moreover, CDON is involved with two of the three major HPE pathways (Massagué, 2003; Rezaei et al., 2012), Nodal and HH. How CDON functions to regulate Nodal signaling is of obvious interest. *Cdon;Lrp2* double mutant mice display phenotypes that resemble Nodal pathway hypomorphs, and CDON and LRP2 each bind to Cripto. Therefore, as with the effects of EtOH, Cripto is a possible point of regulation. One potential mechanism is that CDON and LRP2 might function as components of a larger Nodal receptor complex, contributing via interaction with Cripto. Alternatively, they may work with Cripto in processing and trafficking of Nodal or other receptor components, or play a role in processing and trafficking of Cripto itself (Constam, 2009). There is evidence in other systems that CDON and LRP2 can act in such a manner. LRP2 is best understood as an endocytic receptor that controls internalization and intracellular trafficking of both soluble and membrane-bound proteins, including PTCH1, the Na^+/H^+ exchanger NHE3, and the intrinsic factor receptor, cubilin (Willnow and Christ, 2017). Furthermore, CDON regulates subcellular localization of N-cadherin during neural crest migration in zebrafish (Powell et al., 2015). Similarly, the *Drosophila* orthologs of CDON act not only as co-receptors for HH, but in trafficking of the primary HH receptor, PTC (Zheng et al., 2010). Another possibility is in regulation of cell-cell contact and adhesion. CDON is localized to sites of cell-cell contact and functions with N-cadherin in cell adhesion-dependent signaling (Kang et al., 2003; Lu and Krauss, 2010). In zebrafish, a positive feedback loop exists between Nodal signaling, E-cadherin expression, and duration of cell-cell contact that directs PCP specification, at the expense of endoderm specification (Barone et al., 2017). It is conceivable that CDON could play a role in adhesion-mediated, higher order regulatory events like this as well.

Future work will allow sorting out of these varied, but non-mutually exclusive, mechanisms.

Our findings offer insight into how *Cdon* mutation synergizes with fetal alcohol in mice to produce a wide spectrum of HPE phenotypes, closely resembling the complex etiology and variable outcomes seen in humans at the population level. A combination of approaches, including window of sensitivity studies, genetic interactions in mice, and *in vitro* analyses revealed that, unexpectedly, the point of synergy is at the level of Nodal, not HH, signaling. These findings illuminate gene-environment interactions in the causation of a common birth defect and serve as a conceptual framework for additional developmental anomalies.

METHODS

Mice

All animal procedures were conducted in accordance with institutional guidelines for the care and use of laboratory animals as approved by the Institutional Animal Care and Use Committee (IACUC) of the Icahn School of Medicine at Mount Sinai and according to Max-Delbruck-Center guidelines following approval by local authorities (X9007/17). B6.129P2-*Lefty2*^{tm1Hmd} mice were provided by Hiroshi Hamada. *Cripto-LacZ* mice were provided by Michael Shen. Both strains were transferred onto the 129S6/SvEvTac (129S6) background with the Taconic Speed Congenic Program, by backcrossing and mapping with the 1450 SNP array. Mice used for these experiments were estimated to be over 98% 129S6/SvEvTac background. These lines were crossed with *Cdon*$^{+/tm1Rsk}$ (*Cdon*$^{+/-}$) mice on the 129S6 background (Cole and Krauss, 2003; Hong and Krauss, 2012) to generate 129S6.*Cdon*$^{+/-}$;*Lefty2*$^{+/-}$ and 129S6.*Cdon*$^{+/-}$*Cripto*$^{+/-}$ double-mutant mice. Offspring of intercrosses of these mice were further crossed (see Tables 2 and 3 for details) and pregnant females treated with EtOH or saline as a control (Hong and Krauss, 2012). Briefly, two- to three-month old mice were mated for one hour in the dark and plugged females were collected. The time of the plug was designated as embryonic day (E) 0.0. Pregnant female mice were injected intraperitoneally twice with 15 μl per g body weight of solution of 30% EtOH in saline (3.48 g/kg) at E7.0 and again 4 hours later, with the exception of studies involving *Cdon;Cripto* mutants. For these experiments, a lower dose of ethanol (25% EtOH in saline, 2.9 g/kg) was used. Saline injections were used as controls.

Mice with targeted gene disruption of *Lrp2* (*Lrp2*^{tm1Her}) have been described (Willnow et al., 1996). *Lrp2*$^{+/tm1Her}$ (*Lrp2*$^{+/-}$) mice were kept on the C57BL/6N genetic background and crossed with *Cdon*$^{+/-}$ mice on the C57BL/6N genetic background. Offspring were further intercrossed, and *Lrp2*$^{+/-}$;*Cdon*$^{+/-}$ mice were subjected to timed mating to collect embryos at the depicted embryonic day. Neither *Cdon*$^{-/-}$ mice nor *Lrp2*$^{-/-}$ mice on the C57BL/6N display anterior truncation phenotypes.

Whole mount in situ hybridization

Whole mount RNA in situ hybridization was performed according to standard protocols (Hong and Krauss, 2012). Briefly, embryos were dissected out and fixed in 4% paraformaldehyde in phosphate-buffered saline (PBS), dehydrated through a graded methanol series, and stored at -20°C. Rehydrated embryos were treated with 10 μg/ml proteinase K (Qiagen) in PBS, 0.1% Tween-20 (PBST) according to stage. Embryos were rinsed with PBST, post-fixed and hybridized with digoxygenin (DIG)-labeled probe in hybridization mix (50% formamide, 1.3x SSC pH 5.0, 5 mM EDTA, 50 μg/ml yeast tRNA, 100 μg/ml heparin, 0.2% Tween-20, and 0.5% CHAPS) overnight at 65°C. They were washed, blocked with 2% Roche blocking reagent, 20% heat-inactivated lamb serum in Tris-buffered saline with 0.1% Tween-20 (TBST) and incubated with alkaline phosphate-conjugated anti-DIG antibody (1:2000, Roche) in blocking buffer overnight at 4°C. After washing with TBST and NTMT (100 mM NaCl, 100 mM Tris pH9.5, 50mM $MgCl_2$, and 0.1% Tween-20), embryos were stained with BM Purple AP substrate (Roche) in the dark. Stained embryos were cleared in 80% glycerol and photographed

with a Jenoptik ProgRes C3 camera attached to Nikon SMZ 1500 stereomicroscope. Captured images were assembled by Helicon Focus software (Helicon Soft).

Mouse epiblast stem cell culture and Western blot analysis

Mouse epiblast stem cells (EpiSC9 cells) were obtained from Jianlong Wang and cultured as described (Huang et al., 2017). Briefly, cells were cultured on 0.1% fibronectin-coated plates (MilliporeSigma, 10 μg/ml/cm^2) in N2B27 media supplemented with 20 ng/ml Activin A (R&D Systems) and 12 ng/ml Fgf2 (R&D Systems). Media were changed daily. EpiScs were treated with EtOH for six hours in fresh EpiSC media with supplements. Cells were harvested with RIPA buffer plus protease inhibitor (Sigma) and phosphatase inhibitor (Sigma). Western blotting was as described (Bae et al., 2009). Images were scanned and quantified using ImageJ software. Statistical significance was calculated using Student's t-test and a cutoff of $p<0.05$. Primary antibodies used for Western blot: mouse Cripto (R&D Systems AF1538), SMAD2 (Cell Signaling #5339), p-SMAD2C (Cell Signaling #3108), p-SMAD2L (Cell Signaling #3104), JNK (Cell Signaling #9252), p-JNK (Cell Signaling #9251), and GAPDH (Cell Signaling #97166).

Protein-protein interactions

Expression vectors encoding soluble, tagged forms of CDON, SHH-N, CD164, ActRIIA, ActRIIB, ALK4, Cripto, and LRP2, and LRP2 mini-receptors that encoded the LRP2 transmembrane and intracellular domains, were constructed by standard methods; details are available on request. HEK293T (293T) cells were cultured in DMEM with 10% FBS and 1x Penicillin/Streptomycin. 293T cells in 10 cm dishes were transfected

with a total of either 2 or 3 μg of plasmid vectors using Effectene reagent (Qiagen). Media were changed to 2% FBS two days after transfection. Conditioned media were harvested five days afterwards. Soluble fusion proteins in conditioned media were quantified by dot blotting with human IgG Fc protein (Jackson ImmunoResearch Laboratories) as a standard, and by alkaline phosphatase (AP) enzyme activity using AP yellow liquid substrate (Sigma). For analysis of CDON-Fc interactions with soluble AP-tagged proteins, the factors were coexpressed in HEK293T cells. For Fc pull down and AP activity assays with CDON-Fc, soluble fusion proteins were incubated with protein G agarose beads (Roche) for 2 hours at 4°C. For analysis of soluble LRP2-Fc mini-receptors interactions with soluble AP-tagged proteins, LRP2 sR1-sR4 and the AP-tagged counterparts were generated separately in individual transfections and CM mixed together. Pull down complexes were washed five times with ice-cold HNTG buffer (20 mM HEPES pH 7.5, 150mM NaCl, 0.1% Triton X-100, 10% glycerol). Endogenous AP was inactivated by heat inactivation. AP activity in pull-down complexes was measured using AP yellow liquid substrate (Sigma). For AP pull down followed by Western blot analysis, soluble fusion proteins were incubated with anti-AP conjugated agarose beads (Sigma) overnight at 4°C. Pull-down complexes were washed five times with HNTG buffer, eluted from the beads by boiling, and separated by SDS-PAGE. Antibody used for Western blot was HRP conjugated goat anti-human Fc.

To test SHH-N interaction with membrane-bound LRP2 mini-receptors, NIH3T3 cells were transfected with the four individual LRP2 mini-receptors encoding transmembrane and intracellular domains and incubated with 20μg/ml GST-SHH-N in the medium for two hours. Cell lysates were immunoprecipitated with polyclonal LRP2

antibody directed against full-length LRP2, and subjected to Western blot analysis with anti-LRP2 and anti-GST antibodies.

ACKNOWLEDGMENTS

We thank Horoshi Hamada for providing *Lefty2* mutant mice and reagents; Michael Shen for providing *Cripto* mutant mice and reagents, and helpful discussions; Zoe Fresquez and Marysia-Kolbe Rieder for technical support; Xin Huang and Jianlong Wang for EpiSC9 cells and advice; Nadeera Wickramasinghe and Nicole Dubois for generous support with cell culture; Steve Farber and Phil Soriano for helpful discussions, and Vivian Lo, Allison Kann, and Maggie Hung for reading the manuscript. This work was supported by NIH grant DE024748 from the National Institute of Dental and Craniofacial Research to R.S.K. and German Research Foundation grant CH1838/1-1 to A. Christ.

REFERENCES

Abe, Y., Kruszka, P., Martinez, A.F., Roessler, E., Shiota, K., Yamada, S., and Muenke, M. (2018). Clinical and Demographic Evaluation of a Holoprosencephaly Cohort From the Kyoto Collection of Human Embryos. Anat Rec *301*, 973-986.

Allen, B.L., Song, J.Y., Izzi, L., Althaus, I.W., Kang, J.-S., Charron, F., R.S. Krauss, R.S., and McMahon, A.P. (2011). Overlapping roles and collective requirement for the co-receptors Gas1, Cdo and Boc in Shh pathway function. Dev Cell *20*, 775-787.

Andersson, O., Reissmann, E., Jörnvall, H., and Ibáñez, C.F. (2006). Synergistic interaction between Gdf1 and Nodal during anterior axis development. Dev Biol *293*, 370-381.

Ang, S.L., and Rossant, J. (1994). HNF-3β is essential for node and notochord formation in mouse development. Cell *78*, 561-574.

Aoto, K., Shikata, Y., Higashiyama, D., Shiota, K., and Motoyama, J. (2008). Fetal ethanol exposure activates protein kinase A and impairs Shh expression in prechordal mesendoderm cells in the pathogenesis of holoprosencephaly. Birth Defects Res A Clin Mol Teratol *82*, 224-231.

Aoto, K., Shikata, Y., Imai, H., Matsumaru, D., Tokunaga, T., Shioda, S., Yamada, G., and Motoyama, J. (2009). Mouse Shh is required for prechordal plate maintenance during brain and craniofacial morphogenesis. Dev Biol *327*, 106-120.

Bae, G.U., Domené, S., Roessler, E., Schachter, K., Kang, J.S., Muenke, M., and Krauss, R.S. (2011). Mutations in CDON, Encoding a Hedgehog Receptor, Result in Holoprosencephaly and Defective Interactions with Other Hedgehog Receptors. Am J Hum Genet *89*, 231-240.

Bae, G.U., Yang, Y.J., Jiang, G., Hong, M., Lee, H.J., Tessier-Lavigne, M., Kang, J.S., and Krauss, R.S. (2009). Neogenin regulates skeletal myofiber size and focal adhesion kinase and extracellular signal-regulated kinase activities in vivo and in vitro. Mol Biol Cell *20*, 4920-4931.

Barone, V., Lang, M., Krens, S.F.G., Pradhan, S.J., Shamipour, S., Sako, K., Sikora, M., Guet, C.C., and Heisenberg, C.-P. (2017). An Effective Feedback Loop between Cell-Cell Contact Duration and Morphogen Signaling Determines Cell Fate. Dev Cell *43*, 198-211.e112.

Beachy, P.A., Hymowitz, S.G., Lazarus, R.A., Leahy, D.J., and Siebold, C. (2010). Interactions between Hedgehog proteins and their binding partners come into view. Genes Dev *15*, 2001-2012.

Belo, J.A., Leyns, L., Yamada, G., and De Robertis, E.M. (1998). The prechordal midline of the chondrocranium is defective in Goosecoid-1 mouse mutants. Mech Dev *72*, 15-25.

Brons, I.G.M., Smithers, L.E., Trotter, M.W.B., Rugg-Gunn, P., Sun, B., Chuva de Sousa Lopes, S.M., Howlett, S.K., Clarkson, A., Ahrlund-Richter, L., Pedersen, R.A.*, et al.* (2007). Derivation of pluripotent epiblast stem cells from mammalian embryos. Nature *448*, 191-195.

Christ, A., Christa, A., Kur, E., Lioubinski, O., Bachmann, S., Willnow, T.E., and Hammes, A. (2012). LRP2 Is an Auxiliary SHH Receptor Required to Condition the Forebrain Ventral Midline for Inductive Signals. Dev Cell *22*, 268-278.

Chu, J., Ding, J., Jeays-Ward, K., Price, S.M., Placzek, M., and Shen, M.M. (2005). Non-cell-autonomous role for Cripto in axial midline formation during vertebrate embryogenesis. Development *132*, 5539-5551.

Cohen, M.M., Jr. (2006). Holoprosencephaly: clinical, anatomic, and molecular dimensions. Birth Defects Res Part A Clin Mol Teratol *76*, 658-673.

Cohen, M.M., Jr. , and Shiota, K. (2002). Teratogenesis of holoprosencephaly. Am J Med Genet *109*, 1-15.

Cole, F., and Krauss, R.S. (2003). Microform holoprosencephaly in mice that lack the Ig superfamily member Cdon. Curr Biol *13*, 411-415.

Constam, D.B. (2009). Riding Shotgun: A Dual Role for the Epidermal Growth Factor-Cripto/FRL-1/Cryptic Protein Cripto in Nodal Trafficking. Traffic *10*, 783-791.

Cordero, D., Marcucio, R., Hu, D., Gaffield, W., Tapadia, M., and Helms, J.A. (2004). Temporal perturbations in sonic hedgehog signaling elicit the spectrum of holoprosencephaly phenotypes. J Clin Invest *114*, 485-494.

Croen, L.A., Shaw, G.M., and Lammer, E.J. (2000). Risk factors for cytogenetically normal holoprosencephaly in California: a population-based case-control study. Am J Med Genet *90*, 320-325.

Croy, J.E., Shin, W.D., Knauer, M.F., Knauer, D.J., and Komives, E.A. (2003). All Three LDL Receptor Homology Regions of the LDL Receptor-Related Protein Bind Multiple Ligands. Biochemistry *42*, 13049-13057.

Ding, J., Yang, L., Yan, Y.T., Chen, A., Desai, N., Wynshaw-Boris, A., and Shen, M.M. (1998). Cripto is required for correct orientation of the anterior-posterior axis in the mouse embryo. Nature *395*, 702-707.

Echelard, Y., Epstein, D.J., St-Jacques, B., Shen, L., Mohler, J., McMahon, J.A., and McMahon, A.P. (1993). Sonic hedgehog, a member of a family of putative signaling molecules, is implicated in the regulation of CNS polarity. Cell *75*, 1417-1430.

Filosa, S., Rivera-Pérez, J.A., Gómez, A.P., Gansmuller, A., Sasaki, H., Behringer, R.R., and Ang, S.L. (1997). Goosecoid and HNF-3β genetically interact to regulate neural tube patterning during mouse embryogenesis. Development *124*, 2843-2854.

Geng, X., and Oliver, G. (2009). Pathogenesis of holoprosencephaly. J Clin Invest *119*, 1403-1413.

Grimm, O.H., and Gurdon, J.B. (2002). Nuclear exclusion of Smad2 is a mechanism leading to loss of competence. Nat Cell Biol *4*, 519-522.

Heit, C., Dong, H., Chen, Y., Shah, Y.M., Thompson, D.C., and Vasiliou, V. (2015). Transgenic Mouse Models for Alcohol Metabolism, Toxicity, and Cancer. Adv Exp Med Biol *815*, 375-387.

Heyne, G.W., Melberg, C.G., Doroodchi, P., Parins, K.F., Kietzman, H.W., Everson, J.L., Ansen-Wilson, L.J., and Lipinski, R.J. (2015). Definition of Critical Periods for Hedgehog Pathway Antagonist-Induced Holoprosencephaly, Cleft Lip, and Cleft Palate. PLOS ONE *10*, e0120517.

Hong, M., and Krauss, R.S. (2012). *Cdo*n mutation and fetal ethanol exposure synergize to produce midline signaling defects and holoprosencephaly spectrum disorders in mice PLOS Genet *8*, e1002999.

Hong, M., and Krauss, R.S. (2013). Rescue of Holoprosencephaly in Fetal Alcohol-Exposed Cdon Mutant Mice by Reduced Gene Dosage of Ptch1. PLOS ONE *8*, e79269.

Hong, M., and Krauss, R.S. (2017). Ethanol itself is a holoprosencephaly-inducing teratogen. PLOS ONE *12*, e0176440.

Hong, M., and Krauss, R.S. (2018). Modeling the complex etiology of holoprosencephaly in mice. Am J Med Genet C *178*, 140-150.

Huang, X., Balmer, S., Yang, F., Fidalgo, M., Li, D., Guallar, D., Hadjantonakis, A.K., and Wang, J. (2017). Zfp281 is essential for mouse epiblast maturation through transcriptional and epigenetic control of Nodal signaling. eLife *6*, e33333.

Izzi, L., Lévesque, M., Morin, S., Laniel, D., Wilkes, B.C., Mille, F., Krauss, R.S., McMahon, A.P., Allen, B.L., and Charron, F. (2011). Boc and Gas1 each form distinct Shh receptor complexes with Ptch1 and are required for Shh-mediated cell proliferation. Dev Cell *20*, 788-801.

Jeong, M.-H., Ho, S.-M., Vuong, T.A., Jo, S.-B., Liu, G., Aaronson, S.A., Leem, Y.-E., and Kang, J.-S. (2014). Cdo suppresses canonical Wnt signalling via interaction with Lrp6 thereby promoting neuronal differentiation. Nat Commun *5*, 5455.

Johnson, C.Y., and Rasmussen, S.A. (2010). Non-genetic risk factors for holoprosencephaly. Am J Med Genet C Semin Med Genet *154C*, 73-85.

Kang, J.-S., Feinleib, J.L., Knox, S., Ketteringham, M.A., and Krauss, R.S. (2003). Promyogenic members of the Ig and cadherin families associate to positively regulate differentiation. Proc Natl Acad Sci (USA) *100*, 3989-3994.

Kang, J.-S., Mulieri, P.J., Hu, Y., Taliana, L., and Krauss, R.S. (2002). BOC, an Ig superfamily member, associates with CDO to positively regulate myogenic differentiation. EMBO J *21*, 114-124.

Kang, J.-S., Yi, M.-J., Zhang, W., Feinleib, J.L., Cole, F., and Krauss, R.S. (2004). Netrins and neogenin promote myotube formation. J Cell Biol *167*, 493-504.

Kiecker, C., and Niehrs, C. (2001). The role of prechordal mesendoderm in neural patterning. Curr Opin Neurobiol *11*, 27-33.

Kietzman, H.W., Everson, J.L., Sulik, K.K., and Lipinski, R.J. (2014). The Teratogenic Effects of Prenatal Ethanol Exposure Are Exacerbated by Sonic Hedgehog or Gli2 Haploinsufficiency in the Mouse. PLOS ONE *9*, e89448.

Kojima, Y., Kaufman-Francis, K., Studdert, J.B., Steiner, K.A., Power, M.D., Loebel, D.A.F., Jones, V., Hor, A., de Alencastro, G., Logan, G.J.*, et al.* (2014). The Transcriptional and Functional Properties of Mouse Epiblast Stem Cells Resemble the Anterior Primitive Streak. Cell Stem Cell *14*, 107-120.

Kong, J.H., Siebold, C., and Rohatgi, R. (2019). Biochemical mechanisms of vertebrate hedgehog signaling. Development *146*, dev166892.
Krauss, R.S. (2007). Holoprosencephaly: new models, new insights. Expert Rev Mol Med *9*, 1-17.

Krauss, R.S., and Hong, M. (2016). Gene–Environment Interactions and the Etiology of Birth Defects. Curr Top Dev Biol *116*, 569-580.

Kretzschmar, M., Doody, J., Timokhina, I., and Massagué, J. (1999). A mechanism of repression of TGFβ/ Smad signaling by oncogenic Ras. Genes Dev *13*, 804-816.

Lacbawan, F., Solomon, B.D., Roessler, E., El-Jaick, K., Domené, S., Vélez, J.I., Zhou, N., Hadley, D., Balog, J.Z., Long, R.*, et al.* (2009). Clinical spectrum of SIX3-associated mutations in holoprosencephaly: correlation between genotype, phenotype and function. Journal of Medical Genetics *46*, 389-398.

Lee, R.T.H., Zhao, Z., and Ingham, P.W. (2016). Hedgehog signalling. Development *143*, 367-372.

Leoncini, E., Baranello, G., Orioli, I.M., Annerén, G., Bakker, M., Bianchi, F., Bower, C., Canfield, M.A., Castilla, E.E., Cocchi, G.*, et al.* (2008). Frequency of holoprosencephaly in the International Clearinghouse Birth Defects Surveillance Systems: searching for population variations. Birth Defects Res A Clin Mol Teratol *82*, 585-591.

Lessard, S.J., MacDonald, T.L., Pathak, P., Han, M.S., Coffey, V.G., Edge, J., Rivas, D.A., Hirshman, M.F., Davis, R.J., and Goodyear, L.J. (2018). JNK regulates muscle remodeling via myostatin/SMAD inhibition. Nat Commun *9*, 3030.

Lowe, L.A., Yamada, S., and Kuehn, M.R. (2001). Genetic dissection of nodal function in patterning the mouse embryo. Development *128*, 1831-1843.

Lu, M., and Krauss, R.S. (2010). N-cadherin ligation, but not Sonic hedgehog binding, initiates Cdo-dependent p38α/β MAPK signaling in skeletal myoblasts. Proc Natl Acad Sci (USA) *107*, 4212-4217.

Lyon, R.C., McComb, J.A., Schreurs, J., and Goldstein, D.B. (1981). A relationship between alcohol intoxication and the disordering of brain membranes by a series of short-chain alcohols. J Pharmacol Exp Ther *218*, 669-675.

Marcucio, R.S., Young, N.M., Hu, D., and Hallgrimsson, B. (2011). Mechanisms that underlie co-variation of the brain and face. Genesis *49*, 177-189.

Massagué, J. (2003). Integration of Smad and MAPK pathways: a link and a linker revisited. Genes Dev *17*, 2993-2997.

McAlhany, R.E., West, J.R., and Miranda, R.C. (2000). Glial-derived neurotrophic factor (GDNF) prevents ethanol-induced apoptosis and JUN kinase phosphorylation. Dev Brain Res *119*, 209-216.

McCarns, S.C., Hansch, C., Caldwell, W.S., Morgan, W.T., Moore, S.K., and Doolittle, D.J. (1997). Correlation between hydrophobicity of short-chain aliphatic alcohols and their ability to alter plasma membrane integrity. Fundam Appl Toxicol *36*, 62-70.

McCarthy, N., Wetherill, L., Lovely, C.B., Swartz, M.E., Foroud, T.M., and Eberhart, J.K. (2013). Pdgfra protects against ethanol-induced craniofacial defects in a zebrafish model of FASD. Development *140*, 3254-3265.

McCarthy, R.A., Barth, J.L., Chintalapudi, M.R., Knaak, C., and Argraves, W.S. (2002). Megalin functions as an endocytic sonic hedgehog receptor. J Biol Chem *277*, 25660-25667.

McMahon, A.P., Ingham, P.W., and Tabin, C.J. (2003). Developmental roles and clinical significance of hedgehog signaling. Curr Top Dev Biol *53*, 1-114.

Meno, C., Gritsman, K., Ohishi, S., Ohfuji, Y., Heckscher, E., Mochida, K., Shimono, A., Kondoh, H., Talbot, W.S., Robertson, E.J.*, et al.* (1999). Mouse Lefty2 and Zebrafish Antivin Are Feedback Inhibitors of Nodal Signaling during Vertebrate Gastrulation. Molecular Cell *4*, 287-298.

Miller, E.A., Rasmussen, S.A., Siega-Riz, A.M., Frías, J.L., Honein, M.A., and Study., N.B.D.P. (2010). Risk factors for non-syndromic holoprosencephaly in the National Birth Defects Prevention Study. Am J Med Genet C Semin Med Genet *154C*, 62-72.

Muenke, M., and Beachy, P.A. (2001). Holoprosencephaly. In The Metabolic & Molecular Bases of Inherited Disease, C.R. Scriver, A.L. Beaudet, W.S. Sly, and D. Valle, eds. (New York: McGraw-Hill), pp. 6203-6230.

Mulieri, P.J., Okada, A., Sassoon, D.A., McConnell, S.K., and Krauss, R.S. (2000). Developmental expression pattern of the *cdo* gene. Dev Dyn *219*, 40-49.

Mulieri, P.M., Kang, J.-S., Sassoon, D.A., and Krauss, R.S. (2002). Expression of the *boc* gene during murine embryogenesis. Dev Dyn *223*, 379-388.

Najm, F.J., Chenoweth, J.G., Anderson, P.D., Nadeau, J.H., Redline, R.W., McKay, R.D.G., and Tesar, P.J. (2011). Isolation of Epiblast Stem Cells from Preimplantation Mouse Embryos. Cell Stem Cell *8*, 318-325.

Nomura, M., and Li, E. (1998). Smad2 role in mesoderm formation, left-right patterning and craniofacial development. Nature *393*, 786-790.

Petrov, K., Wierbowski, B.M., and Salic, A. (2017). Sending and Receiving Hedgehog Signals. Annu Rev Cell Dev Biol *33*, 145-168.

Powell, D.R., Williams, J.S., Hernandez-Lagunas, L., Salcedo, E., O'Brien, J.H., and Artinger, K.B. (2015). Cdon promotes neural crest migration by regulating N-cadherin localization. Dev Biol *407*, 289-299.

Ren, Z., Wang, X., Yang, F., Xu, M., Frank, J.A., Wang, H., Wang, S., Ke, Z., and Luo, J. (2017). Ethanol-induced damage to the developing spinal cord: The involvement of CCR2 signaling. Biochim Biophys Acta Mol Basis Dis *1863*, 2746-2761.

Rezaei, H.B., Kamato, D., Ansari, G., Osman, N., and Little, P.J. (2012). Cell biology of Smad2/3 linker region phosphorylation in vascular smooth muscle. Clin Exp Pharmacol Physiol *39*, 661-667.

Robertson, E.J. (2014). Dose-dependent Nodal/Smad signals pattern the early mouse embryo. Semin Cell Dev Biol *32*, 73-79.

Roessler, E., Hu, P., Marino, J., Hong, S., Hart, R., Berger, S., Martinez, A., Abe, Y., Kruszka, P., Thomas, J.W.*, et al.* (2018a). Common genetic causes of holoprosencephaly are limited to a small set of evolutionarily conserved driver genes of midline development coordinated by TGF-β, hedgehog, and FGF signaling. Hum Mutat *39*, 1416-1427.

Roessler, E., Hu, P., and Muenke, M. (2018b). Holoprosencephaly in the genomics era. Am J Med Genet C *178*, 165-174.

Roessler, E., Vélez, J.I., Zhou, N., and Muenke, M. (2012). Utilizing prospective sequence analysis of SHH, ZIC2, SIX3 and TGIF in holoprosencephaly probands to describe the parameters limiting the observed frequency of mutant gene×gene interactions. Mol Genet Metab *105*, 658-664.

Rubenstein, J.L., and Beachy, P.A. (1998). Patterning of the embryonic forebrain. Curr Opin Neurobiol *8*, 18-26.

Sanchez-Arrones, L., Cardozo, M., Nieto-Lopez, F., and Bovolenta, P. (2012). Cdon and Boc: Two transmembrane proteins implicated in cell–cell communication. Int J Biochem Cell Biol *44*, 698-702.

Schier, A.F. (2009). Nodal morphogens. Cold Spring Harb Perspect Biol *1*, a003459.

Shen, M.M. (2007). Nodal signaling: developmental roles and regulation. Development *134*, 1023-1034.

Shiota, K., and Yamada, S. (2010). Early pathogenesis of holoprosencephaly. Am J Med Genet C Semin Med Genet *154C*, 22-28.

Solomon, B.D., Bear, K.A., Wyllie, A., Keaton, A.A., Dubourg, C., David, V., Mercier, S., Odent, S., Hehr, U., Paulussen, A.*, et al.* (2012). Genotypic and phenotypic analysis of 396 individuals with mutations in Sonic Hedgehog. Journal of Medical Genetics *49*, 473-479.

Solomon, B.D., Mercier, S., Vélez, J.I., Pineda-Alvarez, D.E., Wyllie, A., Zhou, N., Dubourg, C., David, V., Odent, S., Roessler, E.*, et al.* (2010). Analysis of genotype-phenotype correlations in human holoprosencephaly. Am J Med Genet C Semin Med Genet *154C*, 133-141.

Song, J., Oh, S.P., Schrewe, H., Nomura, M., Lei, H., Okano, M., Gridley, T., and Li, E. (1999). The type II activin receptors are essential for egg cylinder growth, gastrulation, and rostral head development in mice. Dev Biol *213*, 157-169.

Sparrow, D.B., Chapman, G., Smith, A.J., Mattar, M.Z., Major, J.A., O'Reilly, V.C., Saga, Y., Zackai, E.H., Dormans, J.P., Alman, B.A.*, et al.* (2012). A mechanism for gene-environment interaction in the etiology of congenital scoliosis. Cell *149*, 295-306.

Spoelgen, R., Hammes, A., Anzenberger, U., Zechner, D., Andersen, O.M., Jerchow, B., and Willnow, T.E. (2005). LRP2/megalin is required for patterning of the ventral telencephalon. Development *132*, 405-414.

Sulik, K.K., Johnston, M.C., and Webb, M.A. (1981). Fetal alcohol syndrome: embryogenesis in a mouse model. Science *214*, 936-938.

Summers, A.D., Reefhuis, J., Taliano, J., and Rasmussen, S.A. (2018). Nongenetic risk factors for holoprosencephaly: An updated review of the epidemiologic literature. Am J Med Genet C *178*, 151-164.

Tenzen, T., Allen, B.L., Cole, F., Kang, J.-S., Krauss, R.S., and McMahon, A.P. (2006). The cell surface membrane proteins Cdo and Boc are components and targets of the hedgehog signaling pathway and feedback network in mice. Dev Cell *10*, 647-656.

Tsakiridis, A., Huang, Y., Blin, G., Skylaki, S., Wymeersch, F., Osorno, R., Economou, C., Karagianni, E., Zhao, S., Lowell, S.*, et al.* (2014). Distinct Wnt-driven primitive streak-like populations reflect in vivo lineage precursors. Development *141*, 1209-1221.

Vallier, L., Mendjan, S., Brown, S., Chng, Z., Teo, A., Smithers, L.E., Trotter, M.W.B., Cho, C.H.-H., Martinez, A., Rugg-Gunn, P.*, et al.* (2009). Activin/Nodal signalling maintains pluripotency by controlling Nanog expression. Development *136*, 1339-1349.

Willnow, T.E., and Christ, A. (2017). Endocytic receptor LRP2/megalin—of holoprosencephaly and renal Fanconi syndrome. Pflügers Archiv *469*, 907-916.

Willnow, T.E., Christ, A., and Hammes, A. (2012). Endocytic receptor-mediated control of morphogen signaling. Development *139*, 4311-4319.

Willnow, T.E., Hilpert, J., Armstrong, S.A., Rohlmann, A., Hammer, R.E., Burns, D.K., and Herz, J. (1996). Defective forebrain development in mice lacking gp330/megalin. Proc Natl Acad Sci USA *93*, 8460-8464.

Zalc, A., Rattenbach, R., Auradé, F., Cadot, B., and Relaix, F. (2015). Pax3 and Pax7 Play Essential Safeguard Functions against Environmental Stress-Induced Birth Defects. Dev Cell *33*, 56-66.

Zhang, W., Kang, J.-S., Cole, F., Yi, M.J., and Krauss, R.S. (2006). Cdo functions at multiple points in the Sonic Hedgehog pathway, and Cdo-deficient mice accurately model human holoprosencephaly. Dev Cell *10*, 657-665.

Zhang, X.M., Ramalho-Santos, M., and McMahon, A.P. (2001). Smoothened mutants reveal redundant roles for Shh and Ihh signaling including regulation of L/R symmetry by the mouse node. Cell *106*, 781-792.

Zheng, X., Mann, R.K., Sever, N., and Beachy, P.A. (2010). Genetic and biochemical definition of the Hedgehog receptor. Genes Dev *24*, 57-71.

Table 1: Time course of EtOH-Induced HPE in *Cdon*$^{-/-}$ Embryos

EtOH treatment:	**E7.25**				**E7.5**	
	Saline		EtOH		EtOH	
Phenotype*	*Cdon*$^{+/-}$	*Cdon*$^{-/-}$	*Cdon*$^{+/-}$	*Cdon*$^{-/-}$	*Cdon*$^{+/-}$	*Cdon*$^{-/-}$
Fused upper lip	0/17	2/14	0/21	13/24**	0/13	0/22
Single nostril	0/17	0/14	0/21	5/24	0/13	0/22
Proboscis	0/17	0/14	0/21	2/24	0/13	0/22

* All embryos with HPE had fused upper lip, a fraction of these showed single nostril and proboscis.

**p=0.0165 by Fisher's two-tailed exact test, when compared to EtOH-treated *Cdon*$^{+/-}$ embryos.

Table 2: *Cripto* Heterozygosity Enhances EtOH-Induced HPE in *Cdon*$^{-/-}$ Embryos

Treatment	Genotype (# embryos with HPE/total (%))*		
	Cdon$^{+/-}$;*Cripto*$^{+/-}$	*Cdon*$^{-/-}$;*Cripto*$^{+/+}$	*Cdon*$^{-/-}$;*Cripto*$^{+/-}$
Saline	0/23 (0%)	0/11 (0%)	2/27 (7.4%)
EtOH (2.9 g/kg)	1/48 (2.1%)	9/32 (28.1%)	31/56 (55.4%)**

* Crosses between the following genotypes were used to generate the genotypes scored above:

Cdon$^{+/-}$;*Cripto*$^{+/-}$ x *Cdon*$^{+/-}$;*Cripto*$^{+/-}$

Cdon$^{+/-}$;*Cripto*$^{+/-}$ x *Cdo-*$^{+/-}$;*Cripto*$^{+/-}$

Cdon$^{+/-}$ x *Cdon*$^{+/-}$;*Cripto*$^{+/-}$

Cdon$^{+/-}$ x *Cdon*$^{-/-}$;*Cripto*$^{+/-}$

Cdon$^{-/-}$ x *Cdon*$^{+/-}$;*Cripto*$^{+/-}$

No HPE was found in offspring genotypes other than those shown.

** p=0.014 by Fisher's two-tailed exact test, when compared to EtOH-treated *Cdon*$^{-/-}$;*Cripto*$^{+/+}$ embryos.

Table 3: *Lefty2* Heterozygosity Supresses EtOH-Induced HPE in *Cdon*$^{-/-}$ Embryos

Treatment	Genotype (# affected/total (%))*			
	Total HPE		Single nostril	
	Cdon$^{-/-}$;*Lefty2*$^{+/+}$	*Cdon*$^{-/-}$;*Lefty2*$^{+/-}$	*Cdon*$^{-/-}$;*Lefty2*$^{+/+}$	*Cdon*$^{-/-}$;*Lefty2*$^{+/-}$
Saline	1/12 (8.3%)	0/10 (0%)	0/12 (0%)	0/10 (0%)
EtOH (3.48 g/kg)	33/47 (70.2%)	26/48 (54.2%)	10/47 (21.3%)	3/48 (6.3%)**

* Crosses between the following genotypes were used to generate the genotypes scored above:

Cdon$^{+/-}$;*Lefty2*$^{+/-}$ x *Cdon*$^{+/-}$;*Lefty2*$^{+/-}$

Cdon$^{+/-}$;*Lefty2*$^{+/-}$ x *Cdo-*$^{+/-}$;*Lefty2*$^{+/-}$

Cdon$^{+/-}$ x *Cdon*$^{+/-}$;*Lefty2*$^{+/-}$

Cdon$^{+/-}$ x *Cdo*$^{-/-}$;*Lefty2*$^{+/-}$

Cdon$^{-/-}$ x *Cdon*$^{+/-}$;*Lefty2*$^{+/-}$

No HPE was found in offspring genotypes other than those shown.

** p=0.04 by Fisher's two-tailed exact test, when compared to EtOH-treated *Cdon*$^{-/-}$;*Lefty2*$^{+/+}$ embryos with a single nostril.

FIGURE LEGENDS

Figure 1. Defective Expression of *Lefty2* at the Primitive Streak Stage of EtOH-Treated *Cdon*$^{-/-}$ Embryos

Whole mount in situ hybridization analyses of *Lefty2* in embryos of the indicated genotype and treatment harvested at E7.25. *Lefty2* expression was decreased specifically in EtOH-treated *Cdon*$^{-/-}$ embryos. Numbers of embryos with similar results: *Cdon*$^{+/-}$ (saline) = 6; *Cdon*$^{+/-}$ (EtOH) = 4; *Cdon*$^{-/-}$ (saline) = 9; *Cdon*$^{-/-}$ (EtOH) = 9. Scale Bar, 200 μm.

Figure 2: Acute EtOH Treatment Diminishes p-SMAD2C Levels and Enhances p-JNK1 and p-SMAD2L Levels in mEpiSCs

(A) Representative Western blot of mEpiSCs treated with the indicated doses of EtOH for 6 hours. GAPDH was used as a loading control. (B) Densitometric quantification of p-SMAD2C levels, relative to total Smad2; p-JNK1 levels, relative to total JNK1; and p-SMAD2L levels, relative to total SMAD2, with the indicated doses of EtOH. N=3 experiments with two biological replicates (as shown in (A)) in each experiment. Values are means +/- SD, *p<0.05, **p<0.01, ***p,0.001.

Figure 3: *Cdon* and *Lrp2* Interact Genetically to Produce HPE and Anterior Truncations in Mice

(A) Whole mount E11.5 embryos of the indicated genotype. Note the loss of anterior head structures in the *Cdon*$^{-/-}$;*Lrp2*$^{-/-}$ embryo (arrow). (B) E18.5 embryos of the indicated genotype in whole mount and alizarin red/alcian blue-stained skeleton preparations.

Note the craniofacial truncation in the *Cdon*$^{-/-}$;*Lrp2*$^{-/-}$ embryos (arrows). (C) Whole mount P0 *Cdon*$^{-/-}$;*Lrp2*$^{-/-}$ embryo showing severe HPE.

Figure 4: CDON and LRP2 Bind to Cripto

(A) The indicated AP-tagged proteins were co-expressed with CDON-Fc, and equivalent amounts of AP proteins in conditioned medium (CM) were pulled down. Levels of CDON-Fc in CM and in the pull down were detected by Western blot. (B) CDON-Fc was pulled down from CM derived from transfections as in (A), the amount of CDON-Fc from various CM normalized, and associated AP enzyme activity quantified. N≥4, repeated at least four times for (A) and (B). Values are means +/- SD, *$p<0.05$, **$p<0.01$. (C) Schematic of full length LRP2 and recombinant mini-receptor variants used. Each mini-receptor spans one of the four repetitive modules of the extracellular receptor domain and was expressed either as soluble ectodomain fragments fused to IgG Fc (designated sR1- sR4) or as a membrane-bound mini-receptor fused to the authentic transmembrane and intracellular domains of LRP2 (designated R1- R4). Soluble ectodomain fragments sR1 – sR4 were studied in panel (D), whereas mini-receptors R1 – R4 were used in panel (E). Amino acid numbers next to the full length receptor polypeptide indicate the extent of individual receptor domains. (D) The indicated Fc-tagged proteins were pulled down from CM derived from transfections as in (A), the amount of Fc-tagged protein from various CM normalized, and associated AP enzyme activity quantified. N=3, repeated three times. (E) Cell transfectants expressing the indicated Lrp2 mini-receptor were incubated with GST-SHH-N, and cell lysates

immunoprecipitated with antibody to LRP2 and blotted with antibodies to LRP2 and GST.

Figure S1. *Cripto* Heterozygosity Enhances, and *Lefty2* Heterozygosity Suppresses EtOH-Induced HPE in *Cdon*$^{-/-}$ Embryos

(A) Frontal views of E14.0 embryos. Removal of one copy of *Cripto* enhanced the response of *Cdon*$^{-/-}$ embryos to a dose of 2.9 g/kg EtOH (see Table 2 for quantification). The EtOH-treated *Cdon*$^{-/-}$*;Cripto*$^{+/-}$ embryo displays a fused upper lip (arrow). (B) Frontal views of E14.0 embryos. Removal of one copy of *Lefty2* suppressed formation of single nostril in *Cdon*$^{-/-}$ embryos the response to a dose of 3.48 g/kg EtOH (see Table 3 for quantification). The EtOH-treated *Cdon*$^{-/-}$ embryo displays a fused upper lip and single nostril (black arrow), whereas the EtOH-treated *Cdon*$^{-/-}$*;Lefty2*$^{+/-}$ embryo has a fused upper lip and two nostrils (red arrow).

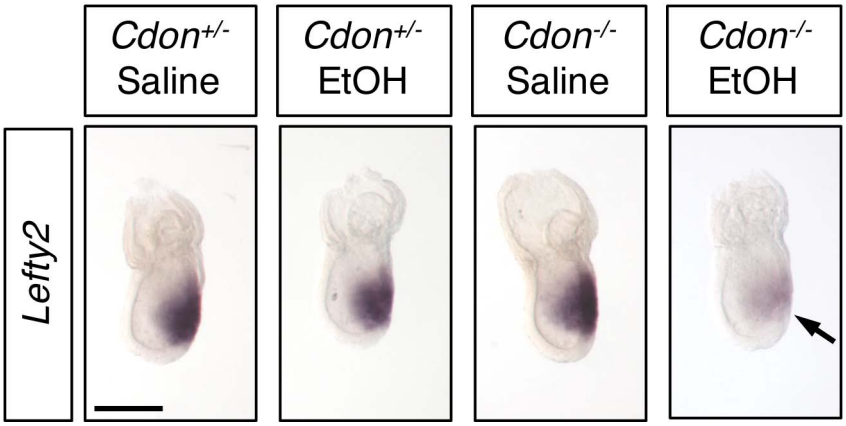

Figure 1

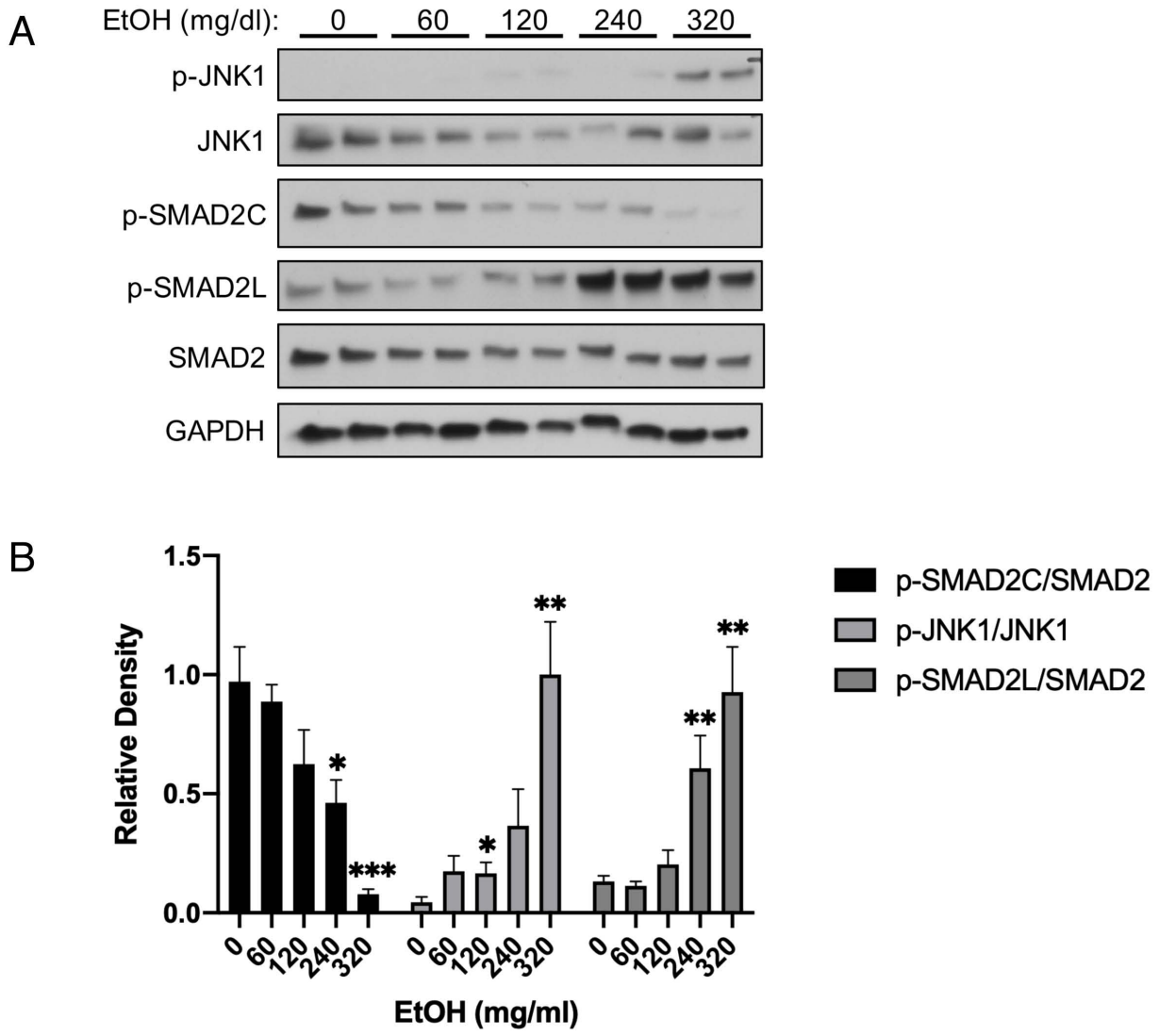
A
EtOH (mg/dl):
0
60
120
240
320
p-JNK1
JNK1
p-SMAD2C
p-SMAD2L
SMAD2
GAPDH
B
Relative Density
1.5
1.0
0.5
0.0
*
***
*
**
**
**
0
60
120
240
320
EtOH (mg/ml)
p-SMAD2C/SMAD2
p-JNK1/JNK1
p-SMAD2L/SMAD2

Figure 2

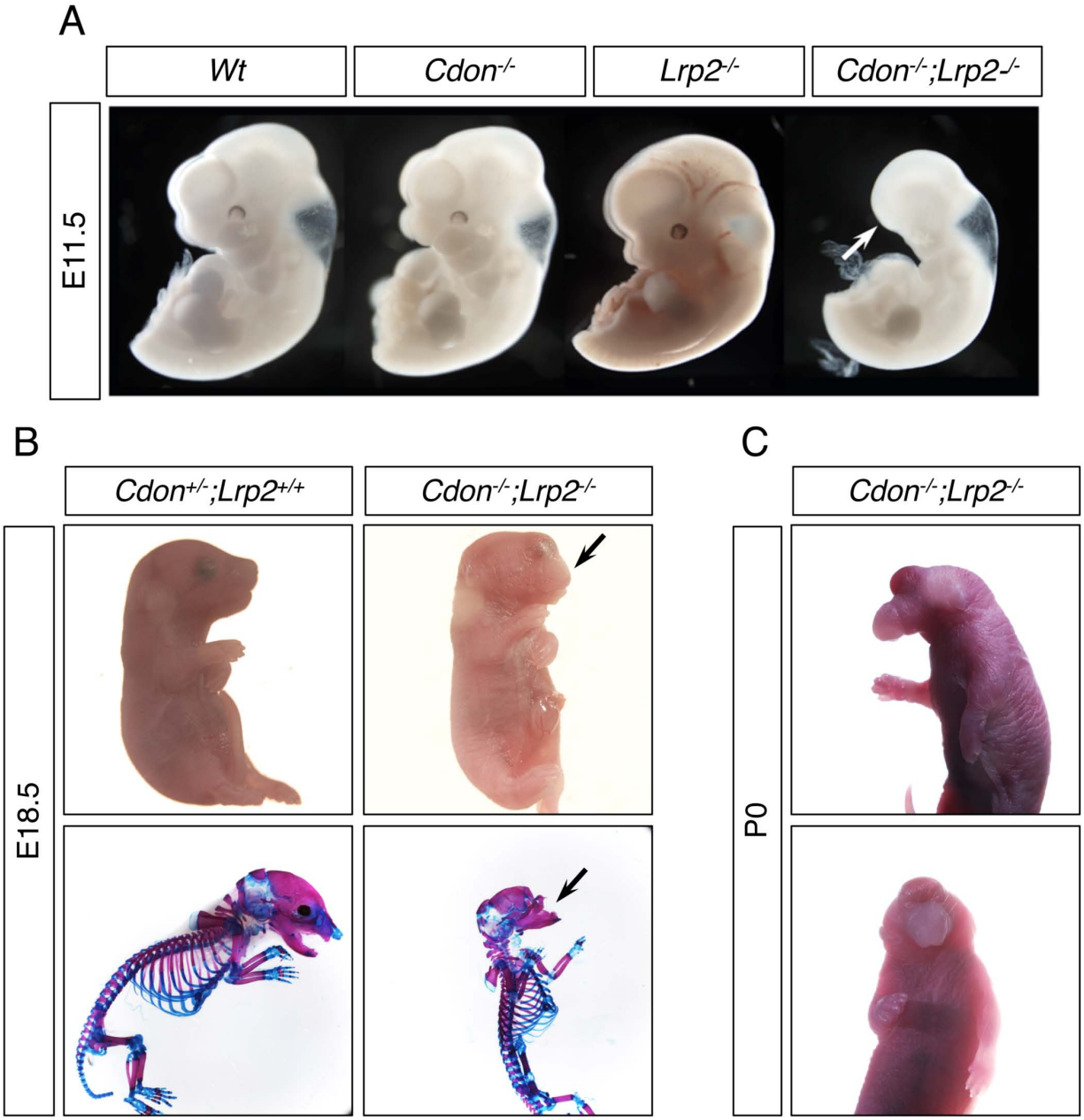
A
Wt
Cdon-/-
Lrp2-/-
Cdon-/-;Lrp2-/-
E11.5
B
Cdon+/-;Lrp2+/+
Cdon-/-;Lrp2-/-
E18.5
C
Cdon-/-;Lrp2-/-
P0

Figure 3

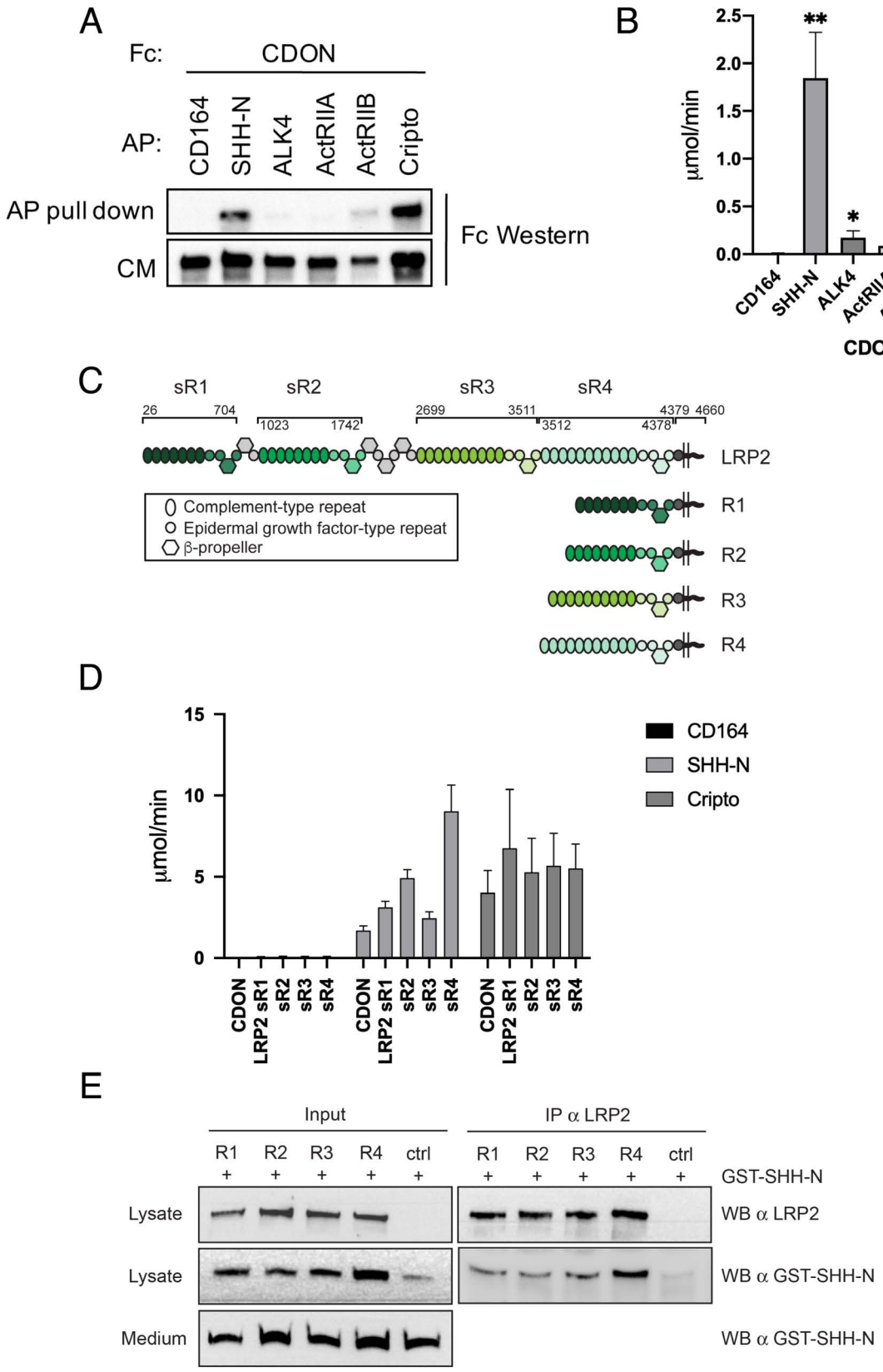
A
Fc:
CDON
AP:
CD164
SHH-N
ALK4
ActRIIA
ActRIIB
Cripto
AP pull down
CM
Fc Western
B
μmol/min
2.5
2.0
1.5
1.0
0.5
0.0
**
*
*
**
**
CD164
SHH-N
ALK4
ActRIIA
ActRIIB
Cripto
CDON
C
sR1
sR2
sR3
sR4
26
704
1023
1742
2699
3511
3512
4378
4379
4660
LRP2
R1
R2
R3
R4
Complement-type repeat
Epidermal growth factor-type repeat
β-propeller
D
μmol/min
15
10
5
0
CD164
SHH-N
Cripto
CDON
LRP2
sR1
sR2
sR3
sR4
E
Input
IP α LRP2
R1
R2
R3
R4
ctrl
GST-SHH-N
Lysate
Lysate
Medium
WB α LRP2
WB α GST-SHH-N
WB α GST-SHH-N

Figure 4

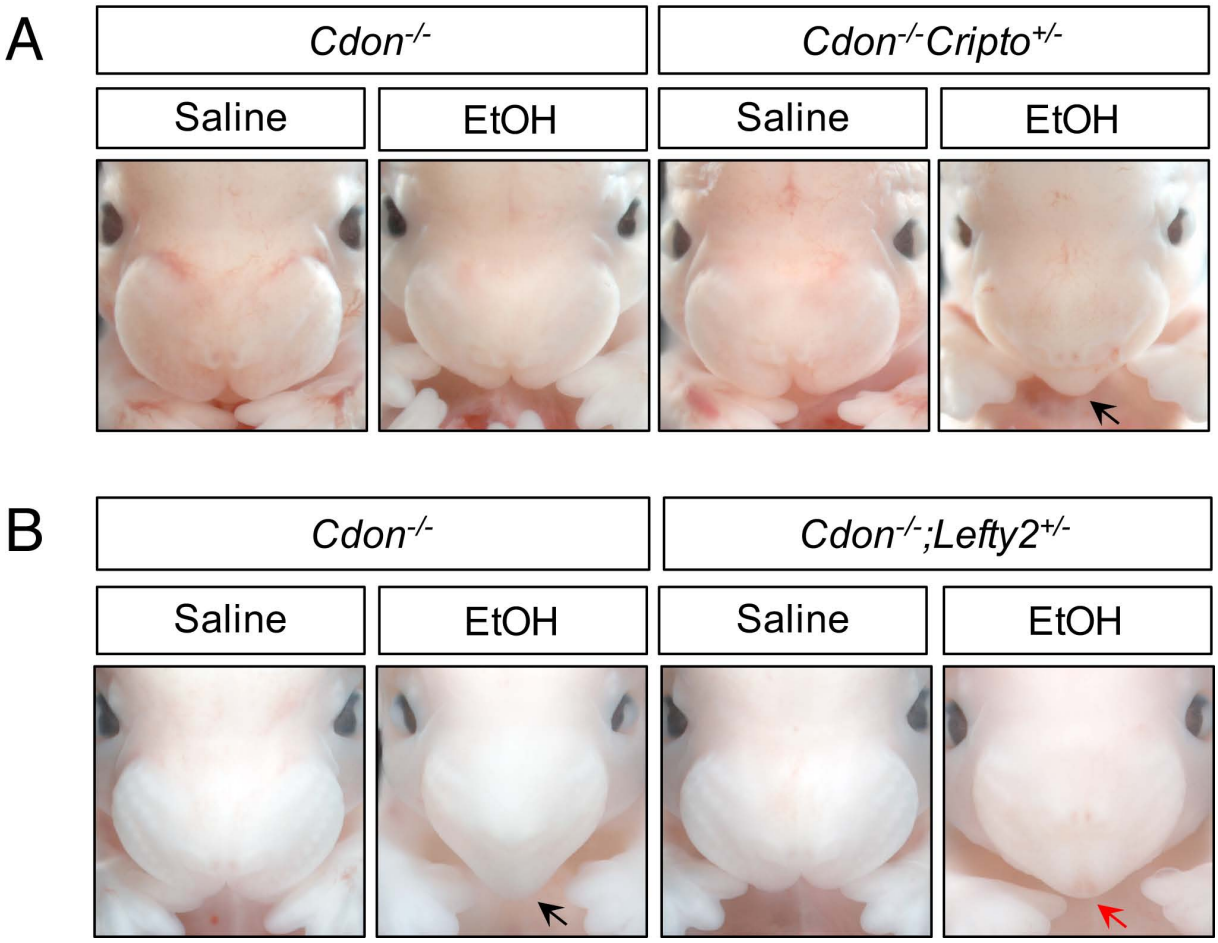
A
Cdon-/-
Cdon-/-Cripto+/-
Saline
EtOH
Saline
EtOH
B
Cdon-/-
Cdon-/-;Lefty2+/-
Saline
EtOH
Saline
EtOH

Figure S1